PHYSICS

Numerical observation of emergent spacetime supersymmetry at quantum criticality

Zi-Xiang Li[1,2], Abolhassan Vaezi[3]*, Christian B. Mendl[4,5], Hong Yao[1,6]*

No definitive evidence of spacetime supersymmetry (SUSY) that transmutes fermions into bosons and vice versa has been revealed in nature so far. Moreover, the question of whether spacetime SUSY in 2 + 1 and higher dimensions can emerge in generic lattice microscopic models remains open. Here, we introduce a lattice realization of a single Dirac fermion in 2 + 1 dimensions with attractive interactions that preserves both time-reversal and chiral symmetries. By performing sign problem–free determinant quantum Monte Carlo simulations, we show that an interacting single Dirac fermion in 2 + 1 dimensions features a superconducting quantum critical point (QCP). We demonstrate that the $\mathcal{N} = 2$ spacetime SUSY in 2 + 1 dimensions emerges at the superconducting QCP by showing that the fermions and bosons have identical anomalous dimensions 1/3, a hallmark of the emergent SUSY. We further show some experimental signatures that may be measured to test such emergent SUSY in candidate systems.

INTRODUCTION

Spacetime supersymmetry (SUSY) was originally proposed as a fundamental symmetry of nature more than four decades ago, but no experimental evidence of SUSY in particle physics has been confirmed. Recently, it has been theoretically argued that SUSY can also spontaneously emerge in certain condensed matter systems (*1*–*14*), e.g., near the superconducting (SC) quantum critical point (QCP) of an interacting single-flavor Dirac fermions in 2 + 1–dimensional (2 + 1D) systems (*5*, *6*). However, verification of this fascinating $\mathcal{N} = 2$ SUSY of a single Dirac fermion in microscopic lattice models in 2 + 1D by nonperturbative and unbiased approaches is still lacking and is thus highly desired.

Dirac fermions are essential ingredients of modern physics that can appear as either elementary particles such as electrons and positrons or emergent quasiparticles, e.g., massless Dirac fermions in graphene and on the surface of 3D topological insulators (*15*, *16*). For a single flavor of massless interacting Dirac fermion in 2 + 1 dimensions, there are numerous interesting phenomena and theoretical predictions, from emergent spacetime SUSY at the SC QCP (*5*, *6*) to the surface topological order (*17*–*20*), as well as fermion dualities (*21*). Although a single Dirac cone can occur on the surface of 3D topological insulators, studying such interacting problems in 2 + 1D microscopic models has been highly challenging due to the notorious no-go theorem of fermion doubling. According to this theorem, it is impossible to realize a single Dirac fermion in local lattice models in two spatial dimensions while maintaining time-reversal and chiral symmetries. Usual lattice regularization of a single-flavor Dirac fermion violates some of those symmetry requirements such that existing approaches cannot reveal many fascinating features associated with a single Dirac fermion.

In this study, we investigate a novel 2D lattice model of spin-1/2 fermions that features a single Dirac point at Γ, with perfectly linear dispersion and quantized π Berry phase around Γ, and preserves both time-reversal and chiral symmetries. Fermions in this model can hop along either the x or y direction, with hopping amplitudes that decay in power law at long distances. At half-filling, namely, when the Fermi level is exactly at the neutral point of single Dirac cone, sufficiently strong attractions between fermions should induce superconductivity in the system. If the lattice regularization can capture low-energy physics of a single Dirac cone, spacetime SUSY could emerge at the SC QCP. Consequently, it is highly desired to investigate universal properties of this putative SC quantum phase transition by a reliable and nonperturbative method like quantum Monte Carlo (QMC) (*22*) without encountering the fermion sign problem (*23*, *24*). However, QMC methods are sign problem free only for limited classes of interacting models (*25*–*32*).

Our lattice model of a single Dirac cone with onsite Hubbard attractive interaction U is sign problem free, which allows us to study the emergent behaviors of the SC quantum phase transition in a numerically reliable way. From the state-of-the-art QMC simulations, we provide convincing evidence that the $\mathcal{N} = 2$ spacetime SUSY emerges at the SC QCP, as shown schematically in Fig. 1. First, the fermions and order parameter bosons have identical anomalous dimensions that are consistent with the exact value of 1/3 (*33*) associated with the $\mathcal{N} = 2$ SUSY. Moreover, we obtain the correlation-length exponent $\nu = 0.87 \pm 0.05$, which is consistent with the nearly exact result of 0.917 obtained from conformal bootstrap calculations (*34*) of the $\mathcal{N} = 2$ SUSY in 2 + 1 dimensions. Moreover, our QMC calculations show that the local electronic density of states $\rho(\omega)$ at $\omega \ll 1$ behaves like $\rho(\omega) \propto \omega^a$ with the exponent $a = 1.37 \pm 0.07$, close to the exact value of 4/3 associated with the $\mathcal{N} = 2$ SUSY, which can be measured in experiments such as scanning tunneling microscopy (STM) to test the predicted SUSY.

RESULTS

The single Dirac fermion model

To regularize a single Dirac fermion on the square lattice while preserving both time-reversal and chiral symmetries, we consider the following single-particle Hamiltonian

$$H_0 = \sum_{ij} (t_{ij} c^\dagger_{i\uparrow} c_{j\downarrow} + H.c.) \quad (1)$$

[1]Institute for Advanced Study, Tsinghua University, Beijing 100084, China. [2]Department of Physics, University of California, Berkeley, Berkeley, CA 94720, USA. [3]Department of Physics, Stanford University, Stanford, CA 94305, USA. [4]Stanford Institute for Materials and Energy Sciences, SLAC National Accelerator Laboratory and Stanford University, Menlo Park, CA 94025, USA. [5]Institute of Scientific Computing, Faculty of Mathematics, Technische Universität Dresden, 01069 Dresden, Germany. [6]State Key Laboratory of Low Dimensional Quantum Physics, Tsinghua University, Beijing 100084, China.
*Corresponding author. Email: vaezi@stanford.edu (A.V.); yaohong@tsinghua.edu.cn (H.Y.)

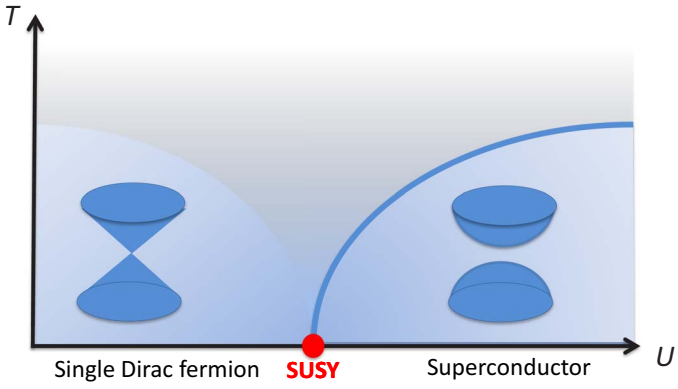

Fig. 1. The phase diagram of a single-flavor Dirac fermion with interactions. From sign problem–free start-of-the-art QMC simulations, we show that the $\mathcal{N} = 2$ spacetime SUSY emerges at the SC QCP. The QMC calculation is performed at zero temperature, and the phase diagram at finite temperature is schematic.

where $c^{\dagger}_{i\sigma}$ creates an electron at site i with spin polarization $\sigma = \uparrow/\downarrow$, and $t_{ij} = t_R$ $(R = r_i - r_j)$ is the hopping amplitude given by

$$t_R = f(R_x, L_x)\delta_{R_y,0} + if(R_y, L_y)\delta_{R_x,0} \quad (2)$$

with $f(R_\alpha, L_\alpha) = i\frac{(-1)^{R_\alpha}}{\frac{L_\alpha}{\pi}\sin\left(\frac{\pi R_\alpha}{L_\alpha}\right)}$, $R_\alpha = 1, \cdots, L_\alpha - 1$, and L_α denoting the number of sites along the $\alpha = x, y$ direction of the square lattice. This type of regularized single Dirac fermion on the lattice was dubbed "SLAC" fermions (*35*). Note that the feature of hopping only along either the x or y direction is not essential, and appropriate hopping along other directions can be added without qualitatively changing the main physics discussed below. We now show that the above lattice model (or SLAC fermion) satisfies all of the requirements expected for a single Dirac fermion for all practical reasons.

It is straightforward to perform a Fourier transform from real to to momentum space and obtain

$$H_0 = \sum_p \psi^{\dagger}_p v_F(p_x\sigma_x + p_y\sigma_y)\psi_p \quad (3)$$

where $\psi_p = (c_{p\uparrow}, c_{p\downarrow})^T$, with $c_{p\sigma}$ annihilating a fermion with momentum $\mathbf{p} = (p_x, p_y)$ and spin σ, v_F is the Fermi velocity (we set $v_F = 1$ hereafter), and σ_a denotes Pauli matrices. Note that the momentum eigenvalues p run over the first Brillouin zone and are quantized as $p_\alpha = \frac{2n\pi}{L_\alpha}$ for periodic boundary conditions. It is clear that the lattice model has a single Dirac point at $\mathbf{p} = 0$ (namely, Γ point) with a linear dispersion all the way to the edges of the first Brillouin zone, as shown in Fig. 2A. Moreover, it can be easily verified that the model does not vary under both time-reversal and chiral symmetries. Note that our model does not directly contradict the fermion-doubling theorem because the hopping here is not local. The hopping amplitudes decay as $1/r$ at long distance.

Besides linear dispersion around the single Dirac point, the lattice model above also exhibits most of the other physical properties expected for Dirac fermions such as π Berry phase around the Dirac point and chiral edge states along mass domain walls. By considering the mass term in the lattice model, namely, $H_0 \to H_0 + m\sum_i c^{\dagger}_i \sigma^z c_i$, it is straightforward to verify that the lattice model gives a Berry phase, which is $\mathrm{sgn}(m)\pi$ for the whole Brillouin zone excluding its boundaries, as shown in Fig. 2B. However, the total Berry phase vanishes due to the $-\mathrm{sgn}(m)\pi$ contribution of the Brillouin zone boundaries. Although this observation seemingly implies the absence of protected zero modes and gapless edge states $|m| > 0$ according to the Atiyah-Singer's index theorem, we shall show below that the edge states along domain walls are nearly gapless with a tiny gap that vanishes as $1/L$, where L is the distance between two domain walls.

We now explicitly consider a domain wall for the mass term along the x direction and periodic boundary condition along the y direction. The local mass term has the following profile: $m(x < L_x/2) = m_0$ and $m(x \geq L_x/2) = -m_0$, where m_0 is a finite constant. In Fig. 2C, the energy eigenvalues are plotted against k_y. Two nearly gapless modes with opposite chiralities appear because of the presence of two domain walls. A direct examination of the single-particle wave functions reveals that the chiral (anti-chiral) branch of edge states is localized around $x = \frac{L_x}{2}$ $(x = L_x)$. For finite L_x, because of the nonzero value of the direct hopping between the two domain walls, the edge states exhibit a tiny gap that decays to zero algebraically ($\propto 1/L_x$), as shown in Fig. 2D. The emergence of the chiral modes along boundaries implies that $C^{\mathrm{eff}}_{m>0} - C^{\mathrm{eff}}_{m<0} = 1$. Recall that $m > 0$ and $m < 0$ regions are time-reversal partners and thus must have opposite Chern numbers, namely, $C^{\mathrm{eff}}_{m>0} = -C^{\mathrm{eff}}_{m<0}$. We thus obtain $C^{\mathrm{eff}}_m = \mathrm{sgn}(m)/2$. Therefore, for all practical reasons, the effective Chern number of the above hopping model can be considered as $\mathrm{sgn}(m)/2$, similar to the surface of 3D topological insulators.

SC quantum criticality

Having shown that the regularized lattice model exhibits almost all physical properties of a single Dirac fermion, we are ready to consider interactions in such a system with the following Hamiltonian

$$H = H_0 + \sum_i U(n_{i\uparrow} - 1/2)(n_{i\downarrow} - 1/2) \quad (4)$$

where U denotes the strength of onsite Hubbard interactions and $n_{i\sigma} = c^{\dagger}_{i\sigma}c_{i\sigma}$. With the onsite Hubbard interactions, the model still respects the particle-hole symmetry such that the system stays at half-filling. When the Hubbard interaction is attractive, namely, $U < 0$, this model is sign problem free in QMC (the details of QMC are discussed in the supplementary materials). Consequently, the interacting effects can be investigated by large-scale numerically reliable QMC simulation. Here, we use projector QMC in the Majorana representation to study the ground-state properties as well as the nature of quantum phase transitions of the model in Eq. 4 with attractive Hubbard interaction. (Previously, quantum criticality was only studied by QMC in 2D Dirac semimetals with even number of Dirac cones.)

It is expected that singlet SC pairing can be generated when the attractive Hubbard interaction is sufficiently strong. To study the quantum phase transition into the putative SC phase, we calculate the structure factor of onsite singlet pairing on a system with size $L \times L$: $S_{\mathrm{SC}}(L) = \frac{1}{L^4}\sum_{ij}\langle\Delta^{\dagger}_i\Delta_j\rangle$, where $\Delta_j = c_{j\downarrow}c_{j\uparrow}$. The SC long-range order can be extracted through finite-size scaling (FSS) $\Delta^2_{\mathrm{SC}} = \lim_{L\to\infty} S_{\mathrm{SC}}(L)$. Besides, we also measure the quasiparticle excitation gap from time-dependent Green's function. From the state-of-the-art QMC simulations (shown in the supplementary materials), we show that the SC order parameter is finite and the single-particle gap is opened when the Hubbard interaction exceeds a critical value.

To accurately identify the QCP, we evaluate the renormalization group (RG)-invariant quantity Binder ratio that is independent of the system

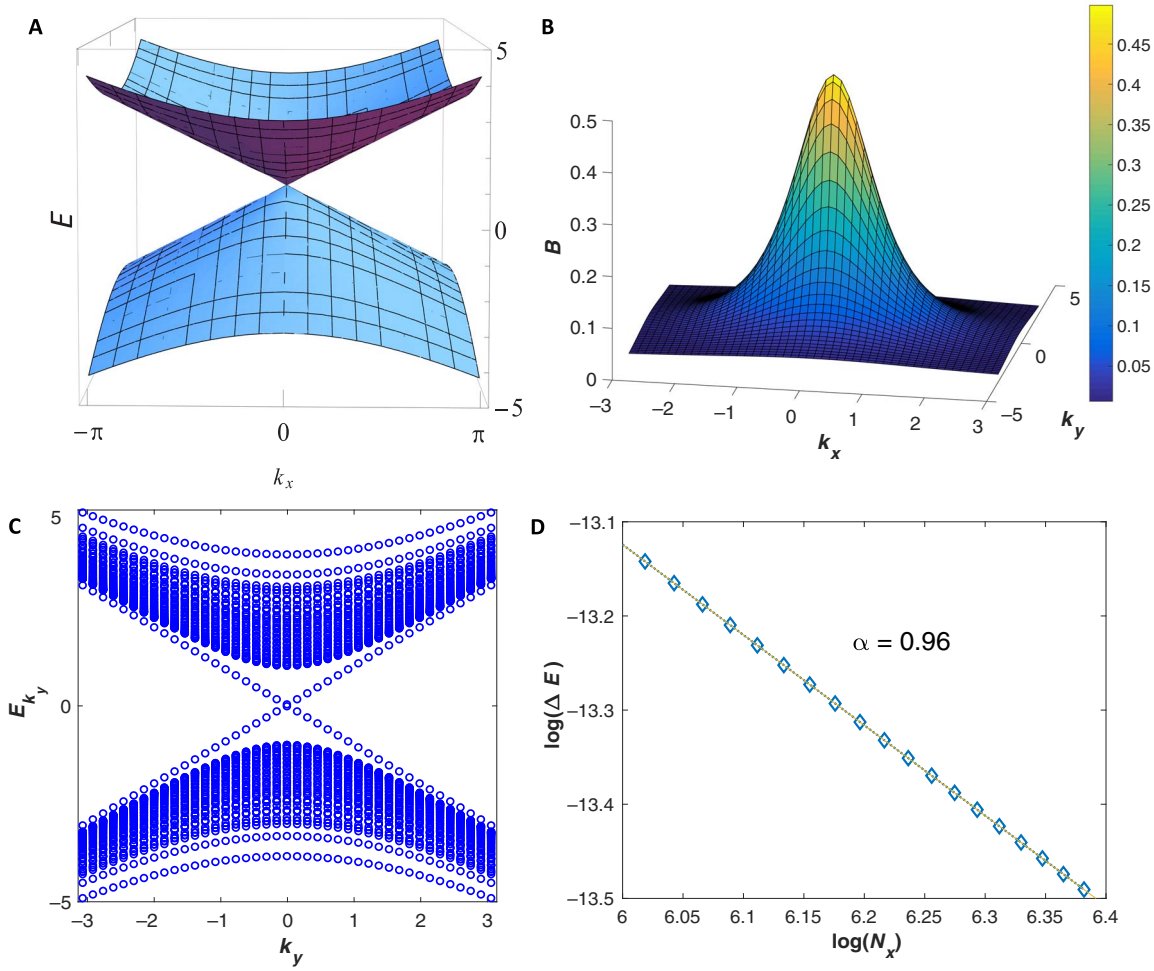

Fig. 2. The band structure of lattice fermions with a single Dirac cone. (**A**) Energy dispersion for a massless lattice Dirac Hamiltonian. The energy dispersion is perfectly linear and given by $E^{\pm}_{k_x,k_y} = \pm|k|$. (**B**) Berry flux of the same model with a finite mass $m = 1$. Although the total Berry phase vanishes, we obtain $\theta_B \simeq \pi$ upon excluding the boundaries of the Brillouin zone. (**C**) We obtain a nearly gapless left-moving (right-moving) boundary state near $x = 0$ ($x = L/2$) by creating a domain wall in the mass term. The results are obtained for $|m| = 1$, and $L_x = L_y = L = 41$. The gap at $k_y = 0$ is nonzero and equal to 0.0483. (**D**) Scaling of the edge-state gap with system size for $|m| = 0.1$. This plot implies that $\Delta E \propto 1/L$ when $m \to 0$.

sizes at the critical point. The Binder ratio is defined as $B = \frac{M_4}{M_2^2}$ where $M_2 \equiv \frac{1}{N^2}\Sigma_{ij}\langle\Delta_i^\dagger\Delta_j\rangle$ and $M_4 \equiv \frac{1}{N^4}\Sigma_{ijkl}\langle\Delta_i^\dagger\Delta_j^\dagger\Delta_k\Delta_l\rangle$ for a system with $N = L^2$ sites. The quantum phase transition point is identified as the crossing point of the Binder ratio for different system sizes L. The results for the Binder ratio, as shown in Fig. 3A, convincingly demonstrate that there is a quantum phase transition from the Dirac semimetal phase to the SC phase occurring at $U = U_c \approx -0.83$ (in unit of the bandwidth). In the SC phase, our QMC calculations show evidences of expected Goldstone modes and Higgs bosons.

Emergent 2 + 1D spacetime SUSY

At the SC QCP $U = U_c$, the system features a single Dirac fermion mode as well as a single complex boson (here, the complex boson is the SC order parameter fluctuation). It was argued from the perturbative renormalization group analysis in $4 - \varepsilon$ spacetime dimensions that a 2 + 1D $\mathcal{N} = 2$ SUSY might emerge by setting $\varepsilon = 1$ (*5*–*7*). However, it is not known a priori whether such spacetime SUSY can emerge in a microscopic model at the QCP and nonperturbative methods such as QMC are needed to address this unambiguously.

If the 2 + 1D $\mathcal{N} = 2$ SUSY emerges at the SC QCP, the anomalous dimensions of fermions and bosons at the QCP should be identical and are equal to 1/3, namely, $\eta_f = \eta_b = \frac{1}{3}$. The equivalence of fermion and boson anomalous dimensions is a hallmark of SUSY. To verify whether the SC QCP in our model features an emergent spacetime SUSY, we study the critical properties of this quantum phase transition systematically through FSS analysis (the details of FSS are shown in the supplementary materials). The anomalous dimensions of the boson and fermion can be extracted via the correlation functions $M_2 \propto \frac{1}{L^{1+\eta_b}}$ and $G_f(L) = \frac{1}{L^2}\Sigma_i\langle c_i^\dagger c_{i+\vec{R}_m} + h.c\rangle \propto \frac{1}{L^{2+\eta_f}}$ according to the definition of anomalous dimensions. Here, $\vec{R}_m = \left(\frac{L-1}{2}, \frac{L-1}{2}\right)$ is the largest separation between two sites in the system.

The bosonic and fermionic correlation functions at the QCP are shown in Fig. 3 (B and C). The anomalous dimensions of the boson and fermion are equal to each other within error bar: $\eta_b = 0.32 \pm 0.02$ and $\eta_f = 0.34 \pm 0.05$. Moreover, the values of the bosonic and fermionic anomalous dimensions obtained from QMC are consistent with the exact result of 1/3 associated with the 2 + 1D $\mathcal{N} = 2$ SUSY. These results provide convincing evidence that the SC QCP in our

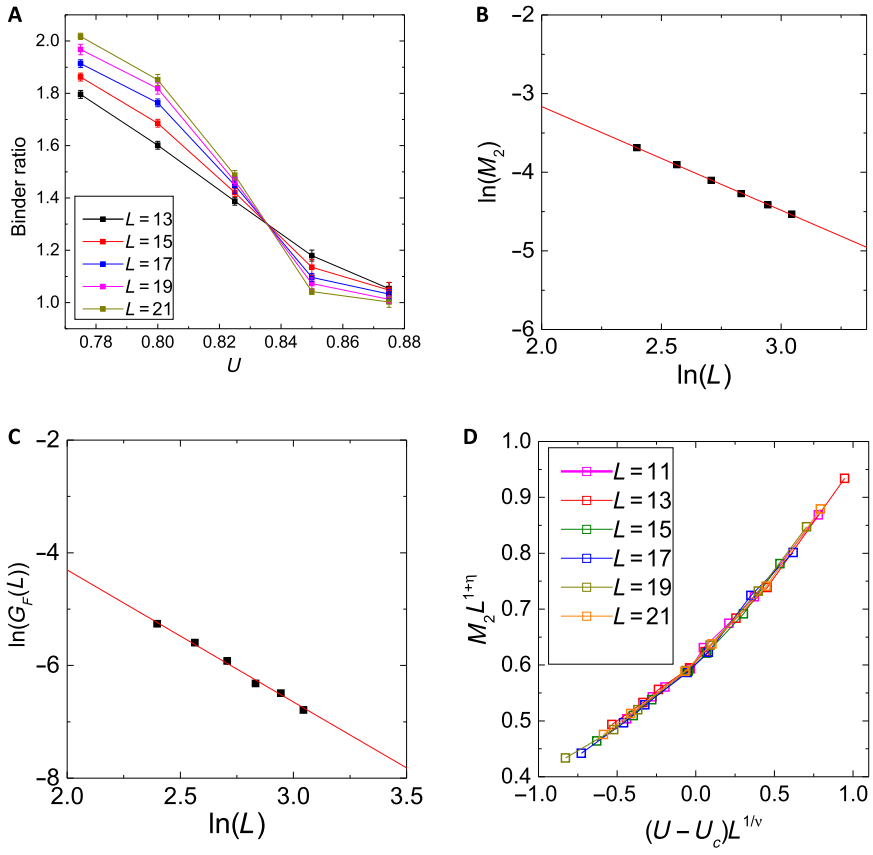

Fig. 3. The QMC results of SC quantum criticality in a single Dirac fermion. (**A**) The Binder ratio results show that SC phase transition occurs at $U_c \approx 0.83$. (**B**) From the structure factor of the SC order parameter plotted versus L, we obtain the boson anomalous dimension $\eta_b = 0.32 \pm 0.02$. (**C**) From the fermion correlation function at largest separation $\vec{R}_m = \left(\frac{L-1}{2}, \frac{L-1}{2}\right)$ plotted versus linear system size L, we obtain fermion anomalous dimension $\eta_f = 0.34 \pm 0.05$. (**D**) By using data collapse analysis of SC structure factors near $U = U_c$ for $L = 11, \cdots, 21$, we obtain the transition point $U_c = 0.827$ and critical exponents $\eta_b = 0.32 \pm 0.02$ and $\nu = 0.87 \pm 0.05$.

regularized lattice model features emergent SUSY. In the supplementary materials, we present the QMC results of bosonic and fermionic correlation functions away from the QCP. It is clear that the boson and fermion anomalous dimensions in the disordered phase away from the QCP are not equal to each other and deviate from 1/3, which indicates that the consistency of the anomalous dimensions between our QMC result and the exact result associated with the $\mathcal{N} = 2$ SUSY theory only occurs at the SC QCP. The consistency between the anomalous dimension of the bosons in the model and the one in the SUSY theory is further supported by the results of the data collapse analysis, as shown in Fig. 3D. In addition, from the data collapse analysis, we extract the correlation-length critical exponent $\nu = 0.87 \pm 0.05$, which is consistent with the nearly exact result of 0.917 obtained from the conformal bootstrap calculation of the $\mathcal{N} = 2$ SUSY theory in 2 + 1D (*34*) and with the results from RG calculations (*36*, *37*). This again indicates that the SC QCP in the interacting quantum model features the emergent spacetime SUSY.

Experimental signatures

The SC QCP of a single Dirac fermion is potentially observable in realistic materials, such as the surface of 3D topological insulators. There are various experimental ways to check the putative emergent SUSY at the SC QCP. For instance, at the QCP, the zero-temperature optical conductivity $\sigma(\omega) = K\frac{e^2}{\hbar}$, where K is a constant known exactly due to the emergent SUSY (*38*). Moreover, the SUSY dictates that the local density of states (LDOS) $\rho(\omega)$ of electrons satisfies the scaling law $\rho(\omega) \propto |\omega|^{\frac{4}{3}}$ for $\omega \ll 1$, which can be measured by STM in experiments. In our model, the LDOS can be calculated by evaluating imaginary-time single-particle Green's function $G_f(\tau) = \langle c_i(0)c_i(\tau)^\dagger \rangle$ in QMC simulations and then performing analytical continuation (see the supplementary materials for details). As shown in Fig. 4A, $G_f(\tau)$ obtained from QMC simulations at the SC QCP behaves as $G_f(\tau) \propto \frac{1}{\tau^\alpha}$ with the exponent $\alpha = 2.34 \pm 0.02$, which is consistent with the one in the $\mathcal{N} = 2$ SUSY. Moreover, by analytical continuation, we obtain the LDOS at SC QCP: $\rho(\omega) \propto |\omega|^a$ with $a \approx 1.37 \pm 0.07$, as shown in Fig. 4B. This scaling of LDOS is consistent with the exact result of 4/3 given by the $\mathcal{N} = 2$ SUSY within error bar. The LDOS can be measured by STM measurements to experimentally test the emergent SUSY.

DISCUSSION

The emergent SUSY observed at the SC QCP in the 2D microscopic model above suggests that the microscopic model can capture all essential physics of a single Dirac cone in 2 + 1D. In particular, it may be used to investigate novel properties of a single Dirac cone on the surface of 3D interacting topological insulators, such as non-Abelian Majorana zero modes at magnetic vortex cones when the single Dirac fermion is SC (*39*). Moreover, it has been recently argued that it is possible to gap out the single Dirac cone surface states of 3D topological insulators without breaking any symmetry through strong interactions, and the

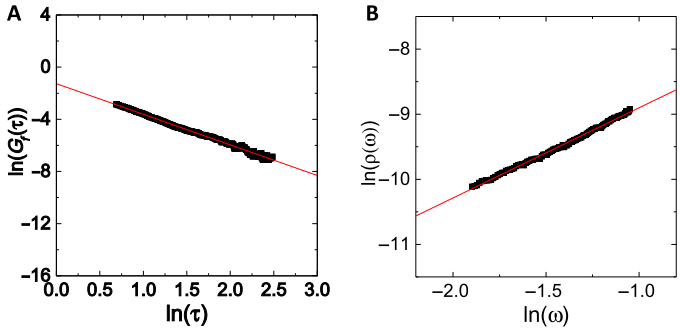

Fig. 4. The QMC results of LDOS and unequal-time single-particle Green's function at SC QCP. (**A**) From the slope of linear fitting in the ln-ln plot of the Green's function versus imaginary time τ, we obtain $G_f(\tau) \propto \frac{1}{\tau^{\alpha}}$, with α = 2.34 ± 0.02. (**B**) From the slope of linear fitting in the ln-ln plot of LDOS versus frequency, we obtain the LDOS $\rho(\omega) \propto |\omega|^a$, with a = 1.37 ± 0.07.

resulting exotic gapped ground state exhibits nontrivial topological order (*17*–*20*). One of the approaches to justifying the quantum phase transition involves disordering the time-reversal symmetric Fu-Kane state via the multiple-vortex proliferation mechanism. We think that adding the interaction $V(\sum_{\langle ij\rangle}\Delta_i^{\dagger}\Delta_j + H.c.)$ with $V > 0$ in Eq. 4 can destroy the SC phase coherence. It would be interesting to study in the future whether such regularized models of a single Dirac fermion can realize the nontrivial surface topological order.

Our work also motivates further studies of other types of 2 + 1D spacetime SUSY in microscopic models by nonperturbative methods. For instance, a sign problem–free microscopic lattice model similar to the one in the present work may be constructed for a single 2 + 1D massless Majorana fermion that can emerge on the surface of 3 + 1D topological superconductors. Strong short-range interactions can gap out Majorana fermions by breaking the time-reversal symmetry, and its QCP may realize an $\mathcal{N} = 1$ SUSY (*5*).

We now discuss distinctions between our work and previous simulations of the supersymmetric Wess-Zumino model [see, e.g., (*40*)]. Previous works mainly investigated lattice regularization of supersymmetric field theories. In contrast, we consider the microscopic lattice model that can mimic the surface of 3D topological insulators with attractive interactions and then investigate whether spacetime SUSY emerges at the SC quantum criticality. Moreover, lattice models studied in previous works are all sign problematic. In contrast, the microscopic lattice model proposed in the present work is sign problem free such that we are able to perform large-scale QMC simulation to reliably verify whether spacetime SUSY emerges at long distance and low energy.

Our unbiased and numerically reliable simulations of the microscopic quantum model of a single Dirac cone have provided convincing evidence of emergent $\mathcal{N} = 2$ spacetime SUSY in 2 + 1 dimensions at the SC QCP. The results presented here can lend concrete support to potentially realize emergent spacetime SUSY in quantum materials such as the surface of 3D topological insulators, e.g., Bi_2Se_3. If realized experimentally, it will not only shed light on the intriguing interplay between topology and symmetry but also provide a promising arena to explore SUSY as well as its spontaneous breaking.

METHODS

Quantum Monte Carlo

We used projector QMC to investigate the ground-state properties of the model of single Dirac fermion described by the Hamiltonian in Eq. 1 with attractive Hubbard interaction. In the projector QMC, the expectation value of an observable O in the ground state can be evaluated as $\frac{\langle\psi_0|O|\psi_0\rangle}{\langle\psi_0|\psi_0\rangle} = \lim_{\Theta\to\infty}\frac{\langle\psi_T|e^{-\Theta H}Oe^{-\Theta H}|\psi_T\rangle}{\langle\psi_T|e^{-2\Theta H}|\psi_T\rangle}$, where ψ_0 is the true ground-state wave function and $|\psi_T\rangle$ is a trial wave function that should have a finite overlap with the true ground-state wave function. Note that Θ is a projection parameter in the simulation. Although $\Theta \to \infty$ is needed to reach the exact ground state, in numerical calculations a sufficient large Θ works for practical purposes of obtaining physical quantities with required accuracy. Because of the absence of sign problem, we can perform large-scale QMC simulations with large system sizes and sufficiently large Θ values. In our QMC simulation, we used periodic boundary condition on the square lattice $L \times L$ with largest $L = 21$. The imaginary-time projection parameter is $2\Theta = 60/t$ for most systems in the calculation. In the calculation of single-particle gap, the systems with large sizes were computed using $2\Theta = 70/t$. We have checked that all the results stayed nearly the same when larger Θ values were used, which ensured desired convergence to the limit of $\Theta \to \infty$.

Because the computational complexity of the determinant QMC algorithm scales in cubic power with the system's volume, it is highly challenging to simulate a fermionic lattice model with a very large size by QMC. Our sign problem–free QMC simulation studied the fermionic model with the largest size accessible within a reasonable computation time. Note that, although numerical results obtained from simulating fermionic models with finite system sizes could have a certain degree of uncertainty, the numerical evidences of emergent SUSY provided by our state-of-the-art QMC simulations are already convincing. It is partly because the raw data obtained from determinant QMC typically have a small statistical error. Moreover, the results of critical exponents extracted from different FSS methods are consistent with each other within error bars, which also indicate that the critical exponents obtained by our QMC simulations are reliable.

SUPPLEMENTARY MATERIALS

Supplementary material for this article is available at http://advances.sciencemag.org/cgi/content/full/4/11/eaau1463/DC1

Supplementary Text

Fig. S1. The QMC results of superconductivity structure factors and single-particle gaps.

Fig. S2. The scaling behaviors of superconductivity structure factors and fermion correlation away from the QCP.

REFERENCES AND NOTES

1. D. Friedan, Z. Qiu, S. Shenker, Conformal invariance, unitarity, and critical exponents in two dimensions. *Phys. Rev. Lett.* **52**, 1575–1578 (1984).
2. L. Balents, M. P. A. Fisher, C. Nayak, Nodal liquid theory of the pseudo-gap phase of high-T_c superconductors. *Int. J. Mod. Phys. B* **12**, 1033–1068 (1998).
3. P. Fendley, K. Schoutens, J. de Boer, Lattice models with $\mathcal{N} = 2$ supersymmetry. *Phys. Rev. Lett.* **90**, 120402 (2003).
4. S.-S. Lee, Emergence of supersymmetry at a critical point of a lattice model. *Phys. Rev. B* **76**, 075103 (2007).
5. T. Grover, D. N. Sheng, A. Vishwanath, Emergent space-time supersymmetry at the boundary of a topological phase. *Science* **344**, 280–283 (2014).
6. P. Ponte, S.-S. Lee, Emergence of supersymmetry on the surface of three-dimensional topological insulators. *New J. Phys.* **16**, 013044 (2014).
7. S.-K. Jian, Y.-F. Jiang, H. Yao, Emergent spacetime supersymmetry in 3D Weyl semimetals and 2D Dirac semimetals. *Phys. Rev. Lett.* **114**, 237001 (2015).
8. S.-K. Jian, C.-H. Lin, J. Maciejko, H. Yao, Emergence of supersymmetric quantum electrodynamics. *Phys. Rev. Lett.* **118**, 166802 (2017).
9. Z.-X. Li, Y.-F. Jiang, H. Yao, Edge quantum criticality and emergent supersymmetry in topological phases. *Phys. Rev. Lett.* **119**, 107202 (2017).
10. A. Rahmani, X. Zhu, M. Franz, I. Affleck, Emergent supersymmetry from strongly interacting Majorana zero modes. *Phys. Rev. Lett.* **115**, 166401 (2015).

11. L. Huijse, B. Bauer, E. Berg, Emergent supersymmetry at the Ising–Berezinskii-Kosterlitz-Thouless multicritical point. *Phys. Rev. Lett.* **114**, 090404 (2015).
12. B. Bauer, L. Huijse, E. Berg, M. Troyer, K. Schoutens, Supersymmetric multicritical point in a model of lattice fermions. *Phys. Rev. B* **87**, 165145 (2013).
13. Y. Yu, K. Yang, Simulating the Wess-Zumino supersymmetry model in optical lattices. *Phys. Rev. Lett.* **105**, 150605 (2010).
14. T. H. Hsieh, G. B. Halász, T. Grover, All Majorana models with translation symmetry are Supersymmetric. *Phys. Rev. Lett.* **117**, 166802 (2016).
15. M. Z. Hasan, C. L. Kane, *Colloquium*: Topological insulators. *Rev. Mod. Phys.* **82**, 3045–3067 (2010).
16. X.-L. Qi, S.-C. Zhang, Topological insulators and superconductors. *Rev. Mod. Phys.* **83**, 1057–1110 (2011).
17. C. Wang, A. C. Potter, T. Senthil, Gapped symmetry preserving surface state for the electron topological insulator. *Phys. Rev. B* **88**, 115137 (2013).
18. M. A. Metlitski, C. L. Kane, M. P. A. Fisher, Bosonic topological insulator in three dimensions and the statistical Witten effect. *Phys. Rev. B* **88**, 035131 (2013).
19. P. Bonderson, C. Nayak, X.-L. Qi, A time-reversal invariant topological phase at the surface of a 3D topological insulator. *J. Stat. Mech.* **9**, P09016 (2013).
20. L. Fidkowski, X. Chen, A. Vishwanath, Non-Abelian topological order on the surface of a 3D topological superconductor from an exactly solved model. *Phys. Rev. X* **3**, 041016 (2013).
21. D. T. Son, Is the composite fermion a Dirac particle? *Phys. Rev. X* **5**, 031027 (2015).
22. R. Blankenbecler, D. J. Scalapino, R. L. Sugar, Monte Carlo calculations of coupled boson-fermion systems. I. *Phys. Rev. D* **24**, 2278–2286 (1981).
23. S. R. White, D. J. Scalapino, R. L. Sugar, N. E. Bickers, R. T. Scalettar, Attractive and repulsive pairing interaction vertices for the two-dimensional Hubbard model. *Phys. Rev. B* **39**, 839–842 (1989).
24. M. Troyer, U.-J. Wiese, Computational complexity and fundamental limitations to fermionic quantum Monte Carlo simulations. *Phys. Rev. Lett.* **94**, 170201 (2005).
25. C. Wu, S.-C. Zhang, Sufficient condition for absence of the sign problem in the fermionic quantum Monte Carlo algorithm. *Phys. Rev. B* **71**, 155115 (2005).
26. Z.-X. Li, Y.-F. Jiang, H. Yao, Solving the fermion sign problem in quantum Monte Carlo simulations by Majorana representation. *Phys. Rev. B* **91**, 241117 (2015).
27. Z.-X. Li, Y.-F. Jiang, H. Yao, Majorana-time-reversal symmetries: A fundamental principle for sign-problem-free quantum Monte Carlo simulations. *Phys. Rev. Lett.* **117**, 267002 (2016).
28. Z. C. Wei, C. Wu, Y. Li, S. Zhang, T. Xiang, Majorana positivity and the fermion sign problem of quantum Monte Carlo simulations. *Phys. Rev. Lett.* **116**, 250601 (2016).
29. E. Berg, M. A. Metlitski, S. Sachdev, Sign-problem-free quantum Monte Carlo of the onset of antiferromagnetism in metals. *Science* **338**, 1606–1609 (2012).
30. E. F. Huffman, S. Chandrasekharan, Solution to sign problems in half-filled spin-polarized electronic systems. *Phys. Rev. B* **89**, 111101 (2014).
31. S. Chandrasekharan, U.-J. Wiese, Meron-cluster solution of fermion sign problems. *Phys. Rev. Lett.* **83**, 3116–3119 (1999).
32. L. Wang, Y.-H. Liu, M. Iazzi, M. Troyer, G. Harcos, Split orthogonal group: A guiding principle for sign-problem-free fermionic simulations. *Phys. Rev. Lett.* **115**, 250601 (2015).
33. O. Aharony, A. Hanany, K. Intriligator, N. Seiberg, M. J. Strassler, Aspects of $N = 2$ supersymmetric gauge theories in three dimensions. *Nucl. Phys. B* **499**, 67 (1997).
34. N. Bobev, S. El-Showk, D. Mazáč, M. F. Paulos, Bootstrapping the three dimensional supersymmetric Ising model. *Phys. Rev. Lett.* **115**, 051601 (2015).
35. S. D. Drell, M. Weinstein, S. Yankielowicz, Strong-coupling field theories. II. Fermions and gauge fields on a lattice. *Phys. Rev. D* **14**, 1627–1647 (1976).
36. N. Zerf, C.-H. Lin, J. Maciejko, Superconducting quantum criticality of topological surface states at three loops. *Phys. Rev. B* **94**, 205106 (2016).
37. N. Zerf, L. N. Mihaila, P. Marquard, I. F. Herbut, M. M. Scherer, Four-loop critical exponents for the Gross-Neveu-Yukawa models. *Phys. Rev. D* **96**, 096010 (2017).
38. W. Witczak-Krempa, J. Maciejko, Optical conductivity of topological surface states with emergent supersymmetry. *Phys. Rev. Lett.* **116**, 100402 (2016).
39. L. Fu, C. L. Kane, Superconducting proximity effect and Majorana fermions at the surface of a topological insulator. *Phys. Rev. Lett.* **100**, 096407 (2008).
40. D. Kadoh, Recent progress in lattice supersymmetry: From lattice gauge theory to black holes. arXiv:1607.01170 (2016).

Acknowledgments: We would like to thank S. Kivelson and S. Shenker for helpful discussions. **Funding:** This work was supported, in part, by the MOST of China under grant nos. 2016YFA0301001 and 2018YFA0305604 (H.Y.) and by the NSFC under grant no. 11474175 (Z.-X.L. and H.Y.). A.V. was funded by the Gordon and Betty Moore Foundation's EPiQS Initiative through grant GBMF4302, and C.B.M. acknowledges support from the DOE Office of Basic Energy Sciences under grant no. DE-AC02-76SF00515 and from the Alexander von Humboldt Foundation. **Author contributions:** Z.-X.L., A.V., C.B.M., and H.Y. performed research, analyzed data, and wrote the paper. **Competing interests:** The authors declare that they have no competing interests. **Data and materials availability:** All data needed to evaluate the conclusions in the paper are present in the paper and/or the Supplementary Materials. Additional data related to this paper may be requested from the authors.

Submitted 10 May 2018
Accepted 27 September 2018
Published 2 November 2018
10.1126/sciadv.aau1463

Citation: Z.-X. Li, A. Vaezi, C. B. Mendl, H. Yao, Numerical observation of emergent spacetime supersymmetry at quantum criticality. *Sci. Adv.* **4**, eaau1463 (2018).

Science Advances

Numerical observation of emergent spacetime supersymmetry at quantum criticality

Zi-Xiang Li, Abolhassan Vaezi, Christian B. Mendl and Hong Yao

Sci Adv **4** (11), eaau1463.
DOI: 10.1126/sciadv.aau1463